Spatiotemporal distribution of albacore in relation to oceanographic variables in the Indian Ocean

Jintao Wang, Jiangfeng Zhu, Xinjun Chen

College of Marine Sciences, Shanghai Ocean University, Shanghai 201306, China;

Key Laboratory of Sustainable Exploitation of Oceanic Fisheries Resources, Ministry of Education, Shanghai Ocean University, Shanghai 201306, China;

National Engineering Research Centre for Oceanic Fisheries, Shanghai Ocean University, Shanghai 201306, China;

Abstract

The albacore tuna, *Thunnus alalonga*, is an economically important oceanic species widely distributed in the Indian Ocean. In this study, we examined the spatiotemporal distribution of albacore tuna with respect to remote sensing oceanographic variables, including sea surface temperature (SST), gradient SST (GSST) calculated from SST, sea surface sanity (SSS), and chlorophyll-*a* (Chl-*a*) during 2006 – 2016 using longline fishery data from the Indian Ocean Tuna Commission (IOTC). The monthly and yearly gravitational centers of catch per unit effort (CPUE) were calculated to represent the variability of local stock abundance on the fishing ground. Two clusters (concentrated and dispersed) of monthly gravitational centers were classified using K-means method. The distribution-habitat associations were quantitatively evaluated including SST between 20 and 27°C, GSST between 0.2 to 0.8 °C 10 km^{-1}, SSS between 34.5 to 35.5 psu, and Chl *a* between 0.1 and 0.2 mg m^{-3}. Two types of fishing ground, coast upwelling fishing ground (CUFG) and deep-sea frontal fishing ground (DFFG), were defined according to their location and oceanographic habitat. This study improves our understanding of the spatiotemporal dynamics of albacore tuna, which is critical for sustainable management of this important resources in the Indian Ocean.

1 Introduction

Albacore tuna (*Thunnus alalunga*) is one of the important commercial species, accounting for 84% of total catches of temperate tunas, in the Indian Ocean for recent years. The albacore tuna fishery could be divided into small juvenile fish (50 – 90 cm FL) and large adult fish (90 – 140 cm FL) fisheries. Small fish are generally habitat in the temperate latitudes, and taken by surface gears (pole and line, troll), whereas large fish are habitat in tropical and subtropical latitudes, and taken by gillnet and longline (Nikolic et al., 2017). Since 2001, albacore tuna is caught mainly by industrial deep-freezing longline fleets and fresh-tuna fleets, with the majority of catches occurring on the high seas by vessels from Chinese Taipei, Chinese mainland, Japan, and coastal countries, such as Indonesia, Malaysia in the Indian Ocean. After 2005, the annual catches of albacore tuna are stability in about 40, 000 t (IOTC, 2016; Nikolic et al., 2017).

The biology of albacore is currently in progress in the Indian Ocean. It was estimated to mature at approximately 5 years of age (Suda, 1974), and the length at first maturity was estimated at 90 cm FL (Wu and Kuo, 1993). The length at 50% maturity of females at 85.3 cm FL (Dhurmeea et al., 2016). The maximum age estimated is 9 -10 years (Cheng et al., 2012; Lee and Liu, 1992).

The distribution of the albacore tuna is not well known. It is widely distributed in temperate and tropical waters ranged from 5° N to 40° S in the Indian Ocean. It is possible that the area from 5° N to 25° S is the distribution area for adult fish in which spawning area exists in the area from 10° S to 25° S and the feeding water from 30° S to 40° S, with the high fish school density (IOTC, 2008; IOTC, 2016). For migration pattern, it is likely that adult albacore tuna does yearly circular counter-clockwise migrations following the surface currents of south tropical gyre between their tropical spawning and southern feeding zones (IOTC, 2016).

The environmental variables strongly regulate the global distribution and migration of albacore in all oceans based on fishery data, such as sea surface temperature (SST), oxygen, oceanic features (Kimura et al., 1997; Chen et al., 2005; Zainuddin et al., 2008; Sagarminaga and Arrizabalaga, 2010, 2014). But the information for Indian Ocean is insufficient, most of those studies focus on the Pacific and Atlantic Ocean. Only one study suggested that the SST, chlorophyll concentration and surface salinity were significant in the distribution of immature albacore. For mature albacore, only SST was significant in the Indian Ocean by the Chinese Taiwan tuna longline fishery during the period 1979 – 1985 (Chen et al., 2005). Similar results are also found for the albacore tuna in the eastern Indian Ocean (IOTC, 2016).

For the sustainable exploitation and management, there is urgently need of understanding the spatiotemporal distribution pattern and environmental preferences for albacore tuna in the Indian Ocean. In this study, we develop an approach to project the spatiotemporal distribution of albacore tuna in the Indian Ocean using remote sensing environmental variables. We calculate the monthly and yearly gravitational centers of albacore tuna and analyze the relationships between the gravitational centers and environmental variables. We classify and evaluate the types of fishing grounds and associated oceanographic conditions. This study could help improve our understanding of the dynamics of albacore tuna and benefit for sustainable fishery in the Indian Ocean.

2 Materials and Methods

2.1 Fishery data

Commercial longline fishery data operated in the areas between 40° S – 5° N and 30° – 120° E in the Indian Ocean during 1995-2016, including monthly catch (t), effort (hooks), fishing dates (year and month), and fishing locations (longitude and latitude), at the resolution of 5° latitude by 5° longitude were obtained from Indian Ocean Tuna Commission (IOTC, http://www.iotc.org/). A spatial scale of 5° × 5° was defined as a fishing unit, and the catch per unit effort (CPUE) in a fishing unit was calculated by the following equation:

$$U_{t,i,j} = \frac{C_{t,i,j}}{E_{t,i,j}} \times 1000 \qquad (1)$$

Where $U_{t,i,j}$, $C_{t,i,j}$ and $E_{t,i,j}$ were the CPUE, the sum of catches within a fishing unit, and the sum of all fishing hooks within a fishing unit, respectively, at longitude *i*, latitude *j* in time *t*. The yearly nominal CPUE was calculated by changing t from month to year (Wang et al., 2016)

The longitudinal and latitudinal gravitational centers of nominal CPUE (G_X and G_Y) in time *t* were calculated to understand the spatiotemporal distribution of fishing ground of albacore in the Indian Ocean.

$$C_{X,t} \frac{\sum_{i=1}^{K} X_i \times U_{t,i}}{\sum_{i=1}^{K} U_{t,i}} \; (2)$$

$$C_{Y,t} \frac{\sum_{i=1}^{K} Y_i \times U_{t,i}}{\sum_{i=1}^{K} U_{t,i}} \; (3)$$

where X_i is the longitudinal midpoint of the *i*th fishing unit between 30° – 120° E, and Y_i is the latitudinal midpoint of the *i*th fishing unit between 50° S – 10° N. Similarly, the gravitational centers of yearly CPUE were also estimated.

2.2 Remote sensing environmental data

Three remote sensing environmental variables including SST, chlorophyll *a* (Chl *a*) and sea surface salinity (SSS) were used to detect the albacore preferences in fishing ground. The monthly SST and Chl *a* data were downloaded from the NOAA OceanWatch (http://oceanwatch.pifsc.noaa.gov/), and the monthly SSS data were obtained from the IRI/LDEO Climate Data Library (http://iridl.ideo.columbia.edu). The spatial resolutions were 0.25°×0.25°, 0.05°×0.05° and 1°×1/3° for SST, Chl *a* and SSS, respectively. All the environmental data were converted into 5°×5° for each month to correspond to the spatial resolution of the fishery data using the mean function (Wang et al., 2015).

Higher SST gradient (GSST) is an indicator of upwelled water from a deeper layer, convergence zones and fronts, the water with greater nutrient in euphotic zones, which enables enhanced production (Solanki et al. 2003, 2015; Wang et al., 2016). GSST was calculated from SST:

$$G_{i,j} = \sqrt{\frac{(T_{i,j-1} - T_{i,j+1})^2 + (T_{i-1,j} - T_{i+1,j})^2}{2}}$$

where *Gi,j* and *Ti,j* are the values of *GSST* and *SST* at longitude *i*, latitude *j*, respectively.

2.3 Statistical method and K-means clustering

The histogram graphs of high catch data and empirical cumulative distribution function (ECDF) are used for describing the relationship and analyzing the stronger association between oceanographic conditions and fishery abundance (Andrade and Garcia 1999; Reynolds 2003; Zainuddin et al., 2008; Zainuddin 2011; Wang et al., 2016). Usually, the ECDF analysis was conducted based on three functions, the empirical cumulative frequency distribution function, the weighted cumulative distribution function, and the absolute value of the difference between the former two curves (Zainuddien et al., 2008, 2011; Wang et al., 2016). In this study, the oceanographic preferences of SST, GSST, Chl *a*, and SSS for albacore were described by histogram graphs and the CPUE weighted ECDF (CPUE-W) were developed to qualitatively evaluate the stronger preferences between the oceanographic variables and albacore CPUE in the Indian Ocean.

Meanwhile, the K-means method was used to classify the clusters of monthly and yearly gravitational centers. The K-means clustering is a method of vector quantization, originally from signal processing, which is popular for cluster analysis in data mining (Han et al., 2011; Wang et al., 2016). It tends to have a higher accuracy if the starting points and the number of cluster is provided (Kuo et al., 2002). Thus, the values of within-groups sum of squares (WSS) were calculated and plotted against the number of cluster to search the best number of cluster. In practice, the best number of cluster was confirmed at the elbow point, and the starting point in each cluster was selected randomly. The WSS was calculated as

$$WSS = \sum_{i}^{K} \sum_{X \in C_i} (m_i - X)^2 \quad (4)$$

where X is a data point in cluster C_i, and m_i is the representative point for cluster C_i.

3 Results

3.1 spatiotemporal distribution of monthly gravitational centers

Two clusters were classified, and two distribution patterns could be observed for monthly gravitational centers of CPUE during 2005 – 2016 (Fig. 1). Concentrated gravitational centers of CPUE is defined as areas spanning approximately 20° longitude (50° - 70° E) (Fig. 1b, 1c,1h, 1j, 1k, 1l), whereas dispersed gravitational centers of CPUE is of 30 (50° - 80° E) or more degrees longitude (Fig. 1a, 1d, 1e, 1f, 1g, 1i). The position for one cluster is close to island or coast of Madagascar in the Northwest Indian Ocean, whereas another cluster is at deep-sea in the Southeast Indian Ocean except for concentrated fishing ground in 2006 (Fig. 1). Apparently, the deep-sea fishing ground for albacore is in the months of April – July, and the coastal fishing ground is in the months of January – March and August – December (Table 1).

3.2 Clusters of yearly gravitational center

The yearly gravitational centers of Albacore tuna in the Indian Ocean could be classified into three clusters by the "elbow effect" (C-I, C-II, and C-III) (Fig. 2). Cluster C-I with the center at 66.9° E and 25.5° S contained gravities of 2006, 2007, and 2012; cluster C-II with the center at 59.9 °E and 24.4° S contained gravities of 2005, 2009, 2014, 2015, and 2016; cluster C-III with the center at 57.3° E and 22.5° S contained gravities of 2008, 2010, and 2013.

3.3 Preferred oceanographic features for albacore

The frequency of albacore tuna's preference in relation to oceanographic variable showed that there were specific ranges where the albacore tuna tended to concentrate (Fig. 3). The fishing ground of albacore tuna occurred in areas where SST ranged from 17 to 27 °C (Fig. 3a), GSST ranged from 0.0 to 1.0 °C 10 km^{-1} (Fig. 3c), SSS ranged from 34.1 to 35.9 psu (Fig. 3e), and Chl *a* ranged from 0.1 to 0.3 mg m^{-3} (Fig. 3g). Based on the ECDF, the cumulative distribution curves of the oceanographic variables were different and the degrees of the differences between the curves for each variable were statistically significant ($p < 0.05$). The stronger associations between the CPUE and variables occurred where SST was between 20 and 27°C (Figure 2b), GSST was between 0.2 to 0.8 °C 10 km^{-1} (Fig. 3d), SSS was between 34.5 to 35.5 psu (Fig. 3f), and Chl *a* was between 0.1 and 0.2 mg m−3 (Figure 3h).

3.4 Integrated environmental distribution maps

The maps of monthly CPUE overlapped with GSST and isotherms were plotted to observe the influences of environmental factors on the distribution of albacore tuna in the Indian Ocean. Two special scenarios, one for dispersed fishing ground in 2010 and the another one for concentrated fishing ground in 2012, were served to delineate the distribution status (Fig. 4 and 5). Two types of fishing ground could be defined easily. Frontal fishing ground located in the area of isothermal ribbon between 20° S and 35° S; coastal upwelling fishing ground is close to island of Madagascar located at 20° S, 40° E for albacore tuna.

4 Discussions

The moderately exploited albacore tuna is widely distributed in the Indian Ocean (IOTC, 2016). Understanding the dynamics of spatiotemporal distribution with respect to reginal oceanographic environmental variables is essential for the sustainable management of this fishery. Limited researches showed that immature and mature albacore tuna displayed a north-south with counter-clockwise seasonal migration (Chen et al., 2005; IOTC 2016). In this study, the similar results of migration pattern based on the updated data supported this conclusion although the spatiotemporal distribution analysis was not differentiated by immature and mature tunas (Fig. 1). The shifts of monthly gravitational center following the "North-South-North" route from January to December seemed to reflect the migration (Fig. 1). Additionally, there is a clearly counter-clockwise migration for months from Mar to July in the area from 25° S to 35° S, the distribution of monthly gravitational centers close to island of Madagascar is complicated (Fig. 1). According to the geography divisions for immature and mature albacore tunas in the Indian Ocean (the south of 30° S is for the immature, the north of 25° S is for the mature, and the area from 25° to 30° S is for the immature and mature, Nikolic et al., 2017), the operating for albacore longline fishery mostly occurred in the mature area, the operating occurred in the months of April and May located in the immature area (Fig. 1).

Usually, sea surface temperature is served as a significant factor to study the albacore tuna distribution. For example, SST with different ranges appears to be an important predictor of CPUE for immature albacore in surface waters in the Northeastern Atlantic (16° - 18° C) and Northeastern Pacific (14° - 17° C) (Sagarminaga and Arrizabalaga, 2010; Philips et al., 2014). In the Indian Ocean, the SST at high albacore abundance depended on life stage and season. For immature albacore, areas with SST between 15°C and 21°C had higher CPUE; areas with SST between 15°C and 27°C had higher CPUE for mature albacore (Chen et al., 2005). Because of the biological characteristics of albacore tuna, such as thermoregulation (Morrison et al., 1978; Graham and Dickson, 1981), the wide range of stronger preference of SST was detected from 20°C to 27°C, which is consistent with the result derived using fuzzy synthesis approach (Chen et al., 2005).

As for other oceanographic variables used in this study, little attention was given to identifying the stronger preferences for albacore tuna in the Indian Ocean. We used frequency and empirical cumulative distribution function methods to identify the specific range of favorable environmental conditions, which provides the knowledge for albacore tuna in the Indian Ocean.

Two types of fishing ground were defined based on the clusters of monthly gravitational centers and corresponding oceanography, the coastal upwelling fishing ground (CUFG) and deep-sea front fishing ground (DFFG) in Indian Ocean. CUFG is close to coasts and islands of Madagascar and provides productivity by the coastal upwelling system (Nikolic, et al., 2017); DFFG is at the deep-sea and it is main between 20° - 40° S, 60° - 100° E. The integrated environmental distribution maps showed that the area of DFFG mainly occupy by relatively high GSST and isothermal ribbons (Fig. 4 and 5). GSST calculated from remote sensing data is a convenient and effective indicator for the convergence zones and fronts where have high secondary/tertiary productions in the ocean (Polovina et al., 2001; Solanki et al., 2003; Wang et al., 2016). Thus, the fishing ground at the deep sea is supported by the food from the convergence zones and fronts.

In addition, the reasons caused the differences between concentrated and dispersed gravitational center of fishing ground is that the fishing operation for a year mainly occurred in the CUFG. But the deep reasons need to be investigated from fishery oceanography, biology, and ecology of albacore tuna in the Indian Ocean (Corbineau et al., 2008; Nikolic, et al., 2017)

In conclusion, the spatiotemporal distribution and habitat oceanographic characteristics of fishing ground for albacore tuna in the Indian Ocean were identified and the relationships between them were analyzed. The types of fishing ground were defined by the position and the habitat oceanography of fishing ground. The findings would be useful for understanding of spatiotemporal dynamics of albacore with respect to habitat environment. Derived information can be used in fishery management, such as establishment of marine protection area for albacore in the Indian Ocean.

Acknowledgements

The authors thank the Chinese Squid-jigging Technology Group of Shanghai Ocean University for providing the fishery data, thank the NOAA OceanWatch and the IRI/LDEO Climate Data Library for providing the environmental data. This study was financially supported by the National Natural Science Funding of China (NSFC31702343, NSFC41876141).

References

Andrade, H. A., Garcia, C. A. E. 1999. Skipjack Tuna Fishery in Relation to Sea Surface Temperature off the Southern Brazilian Coast. Fisheries Oceanography, 8(4): 245–254.

Chen, I., Lee, P., Tzeng, W. 2005. Distribution of albacore (*Thunnus alalunga*) in the Indian Ocean and its relation to environmental factors. Fisheries Oceanography, 14(1): 71-80.

Cheng, Z., Fengying, L., Hao, T., Liuxiong, X., Siquan, T. 2012. Age and growth of albacore Tuna (*Thunnus alalunga*) in the southern and central Indian Ocean based on Chinese observer data. IOTC, IOTC–2012–WPTmT04–16 Rev_1.

Dhurmeea, Z., Zudaire, I., Chassot, E., Cedras, M., Nikolic, N., Bourjea, J., West, W., Appadoo, C., Bodin, N. 2016. Reproductive biology of albacore tuna (*Thunnus alalunga*) in the Western Indian Ocean. IOTC-2016-WPTmT06-27.

Graham, J.B., Dickson, K.A. 1981. Physiological thermoregulation in the albacore tuna *Thunnus alalunga*. Physiological Zoology, 54:470–486.

Han, J., Kamber, M., Pei, J. 2011. Data Mining: Concepts and Techniques. San Francisco, CA: Elsevier.

Corbineau, A., Rouyer, T., Cazelles, B., Fromentin, J., Fonteneau, A. 2008. Time series analysis of tuna and swordfish catches and climate variability in the Indian Ocean (1968 – 2003). Aquatic Living Resources, 21, 277-285.

IOTC (2008) General reviews of Indian Ocean Albacore (*Thunnus alalunga*). Bangkok, Thailand, 1 Nov 2008, IOTC-2008-WPTe-INF03 [E].

IOTC (2016) Review of the statistical data and fisery trends for albacore. Shanghai, China, 18-21 Jul 2016 IOTC, IOTC–2016–WPTmT06–07 [E].

IOTC (2016) Indian Ocean albacore stock: review of its fishery, biological data and results of its 2014 stock assessment. Shanghai, China, 18-21 Jul 2016 IOTC, IOTC–2016–WPTmT06–09 [E].

IOTC (2016) Albacore supporting information. Shanghai, China, 18-21 Jul 2016 IOTC.

Kimura, S., Nakai, M., Sugimoto, T. 1997. Migration of albacore, *Thunnus alalunga*, in the North Pacific Ocean in relation to large oceanic phenomena. Fisheries Oceanography, 6:51–57.

Kuo, R. J., Ho, L. M., Hu, C. M. 2002. Integration of Self-Organizing Feature Map and K-Means Algorithm for Market Segmentation. Computers & Operations Research 29: 1475–1493.

Lee, Y.C., Liu, H.C. 1992. Age determination, by vertebra reading, in Indian Albacore, *Thunnus alalunga* (Bonnaterre). J Fish Soc Taiwan, 19(2):89–102

Morrison, D.C., Laurs, R.M., Ulevitch, R.C. 1978. Activity of albacore serum complement reflects its thermoregulatory capacity. In: Sharp GD, Dizon AE (eds) The physiological ecology of tunas. Academic Press, New York, pp 141–150.

Nikolic, N., Morandeau, G., Hoarau, L., West, W., Arrizabalaga, H., Hoyle, S., Nicol, J.S., Bourjea, J., Puech, A., Farley, J.H. 2017. Review of albacore tuna, *Thunnus alalunga*, biology, fisheries and management. Reviews in Fish Biology and Fisheries, 27: 775-810.

Philips, A.J., Ciannelli, L., Brodeur, R.D., Pearcy, W.G., Childers, J. 2014. Spatio-temporal associations of albacore CPUEs in the Northeastern Pacific with regional SST and climate environmental variables. ICES Journal of Marine Science, 71(7):1717–1727.

Polovina, J. J., Howell, E., Kobayashi, D. R., Seki, M. P. 2001. The Transition Zone Chlorophyll Front, a Dynamic Global Feature Defining Migration and forage Habitat for Marine Resources. Progress in Oceanography, 49 (1–4): 469–483

Reynolds, J. A. 2003. Quantifying Habitat Associations in Marine Fisheries: A Generalization of the Kolmogorov–Smirnov Statistic Using Commercial Logbook Records Linked to Archived Environmental Data. Canadian Journal of Fisheries and Aquatic Sciences, 60(4): 370–378.

Suda, A. 1974. Recent status of resources of tuna exploited by longline fishery in the Indian Ocean. Bull Fish Res Lab, 10: 27-62.

Sagarminaga, Y., Arrizabalaga, H. 2010. Spatio-temporal distribution of albacore (Thunnus alalunga) catches in the northeastern Atlantic: relationship with the thermal environment. Fisheries Oceanography, 19:121–134.

Sagarminaga, Y., Arrizabalaga, H. 2014. Relationship of Northeast Atlantic albacore juveniles with upper surface thermal and chlorophyll-a fronts. Deep-Sea Res Part II, 107:54–63

Solanki, H. U., Dwivedi, R. M., Nayak, S. R., Somvanshi, V. S., Gulati, D. K., Pattnayak, S. K. 2003. Fishery Forecast Using OCM Chlorophyll Concentration and AVHRR SST: Validation Results off Gujarat Coast, India. International Journal of Remote Sensing 24: 3691–3699.

Solanki, H. U., Bhatpuria, D., Chauhan, P. 2015. Integrative Analysis of AltiKa-SSHa, MODIS-SST,

and OCM-Chlorophyll Signatures for Fisheries Applications. Marine Geodesy, 38: 672–683.

Solanki, H. U., Dwivedi, R. M., Nayak, S. R., Somvanshi, V. S., Gulati, D. K., Pattnayak, S. K. 2003.

Fishery Forecast Using OCM Chlorophyll Concentration and AVHRR SST: Validation Results off Gujarat Coast, India. International Journal of Remote Sensing 24: 3691–3699.

Wu, C.L., Kuo, C.L. 1993. Maturity and fecundity of albacore, *Thunnus alalunga* (Bonnaterre), from the Indian Ocean. J Fish Soc Taiwan, 20(2):135–151

Wang, J., Y, W., Chen, X., Chen, Y. 2015. Detection of potential fishing zones for neon flying squid based on remote sensing data in the Northwest Pacific Ocean using an artificial neural network. International Journal of Remote Sensing, 36(13): 3317-3330.

Wang, J., Chen, X., Chen, Y. 2016. Spatio-temporal distribution of skipjack in relation to oceanographic conditions in the west-central Pacific Ocean. International Journal of Remote Sensing, 37(24): 6149-6164.

Zainuddin, M., Saitoh, K., Saitoh, S.I. 2008. Albacore (Thunnus alalunga) fishing ground in relation to oceanographic conditions in the western North Pacific Ocean using remotely sensed satellite data. Fisheries Oceanography, 17:61–73.

Zainuddin, M. 2011. Skipjack Tuna in Relation to Sea Surface Temperature and Chlorophyll-A

Concentration of Bone Bay Using Remotely Sensed Satellite Data." Jurnal Ilmu dan Teknologi

Kelautan Tropis 3 (1): 82–90

Figure caption

Figure 1 The distribution of monthly gravitational center of CPUE for albacore from 2005 to 2016 in the Indian Ocean. The monthly gravitational center of CPUE for each year could be classified into two clusters (blue and red). The south of 30° S is for the immature albacore tuna, the north of 25° S is for the mature albacore tuna, and the area from 25° to 30° S is the mixed zone for the immature and mature albacore tuna.

Figure 2 (a) The numbers of cluster against the within groups sum of squares (WSS); (b) the clusters for yearly gravitational centers of Albacore from 2005 to 2016 according to 'elbow effect'.

Figure 3 Albacore tuna fishing frequencies in relation to SST (a), GSST (c), SSS (f), Chl *a*(g); empirical cumulative distribution frequencies (black line), monthly CPUE weighted ECDF (red line), the absolute difference between ECDF and CPUE weight ECDF (blue line) for SST (b), GSST (d), SSS (f), Chl *a* (h) during 2005 – 2016.

Figure 4 The distribution of monthly CPUE overlapping GSST and SST isotherm in 2010 for the scenario of dispersed fishing ground.

Figure 5 The distribution of monthly CPUE overlapping GSST and SST isotherm in 2012 for the scenario of concentrated fishing ground.

Tables

Table 1 The months for concentrated and dispersed fishing ground of albacore in the Indian Ocean, respectively. Cluster A was represented by red points and cluster B was represented by blue points in Figure 1.

Distribution patter	Year	Cluster

		Cluster A	Cluster B
Concentrated	2006	1,2,3,8,9,10,11,12	4,5,6.7
	2007	1,2,10,11,12	3,4,5,6,7,8,9
	2012	1,2,3,6,7,8,9,10,11,12	4,5
	2014	1,2,3,8,9,10,11,12	4,5,6,7
	2015	1,2,4,7,8,9,10,11,12	3,5,6
	2016	1,2,7,8,9,10,11,12	3,4,5,6,
Dispersed	2005	1,2,7,8,9,10,11,12	3,4,5,6
	2008	1,2,3,10,11,12	4,5,6,7,8,9
	2009	1,2,8,9,10,11,12	3,4,5,6,7
	2010	1,2,7,8,10,11,12	3,4,5,6,9
	2011	1,2,9,10,11,12	3,4,5,6,7,8
	2013	1,2,3,9,10,11,12	4,5,6,7,8

Figures

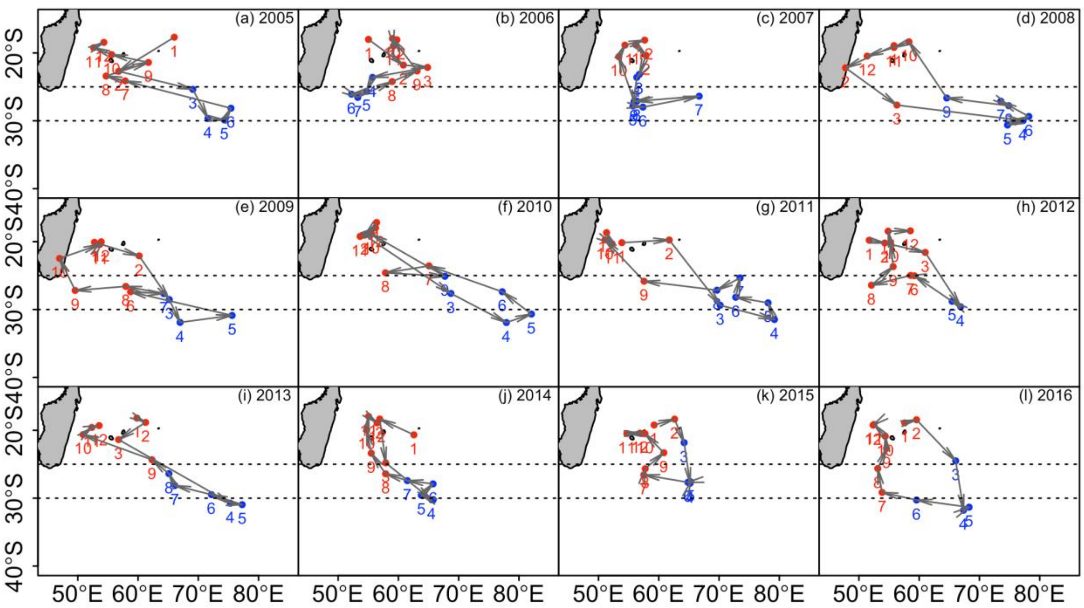

Fig. 1

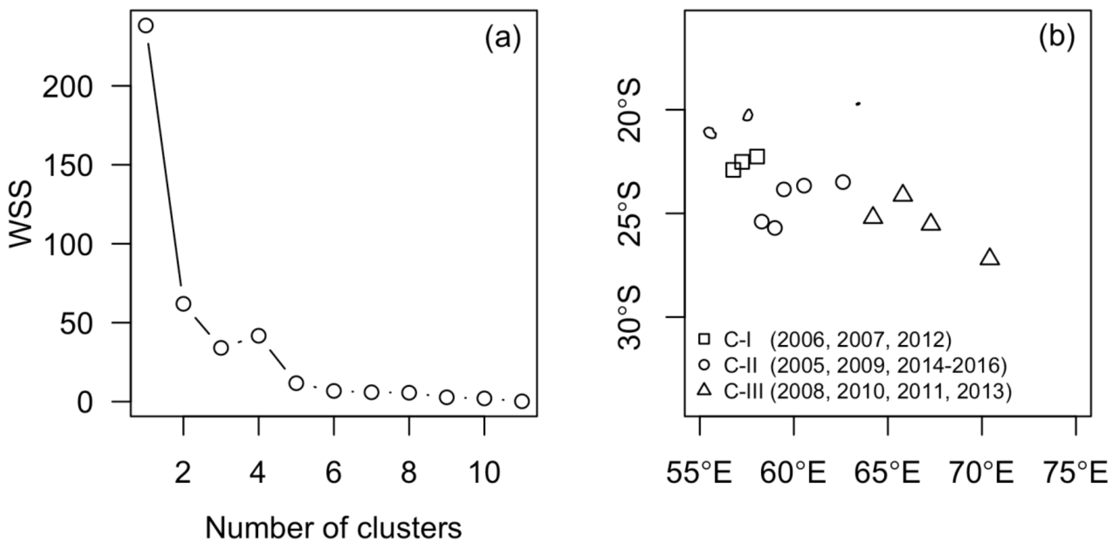
(a)
WSS
200
150
100
50
0
2
4
6
8
10
Number of clusters
(b)
20°S
25°S
30°S
C-I (2006, 2007, 2012)
C-II (2005, 2009, 2014-2016)
C-III (2008, 2010, 2011, 2013)
55°E
60°E
65°E
70°E
75°E

Fig. 2

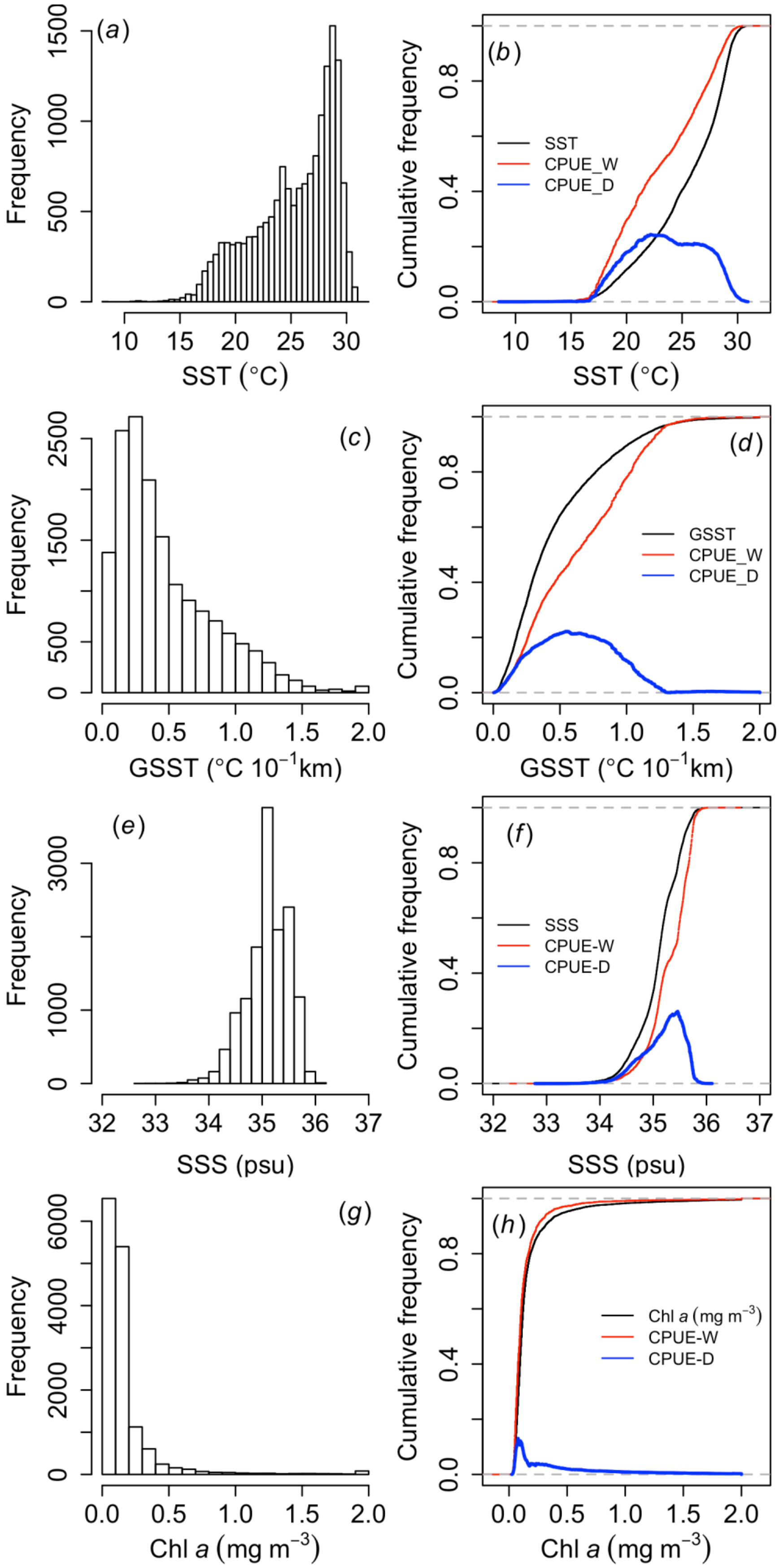

(a)
Frequency
SST (°C)
(b)
Cumulative frequency
SST
CPUE_W
CPUE_D
SST (°C)
(c)
Frequency
GSST (°C 10^{-1}km)
(d)
Cumulative frequency
GSST
CPUE_W
CPUE_D
GSST (°C 10^{-1}km)
(e)
Frequency
SSS (psu)
(f)
Cumulative frequency
SSS
CPUE-W
CPUE-D
SSS (psu)
(g)
Frequency
Chl a (mg m^{-3})
(h)
Cumulative frequency
Chl a (mg m^{-3})
CPUE-W
CPUE-D
Chl a (mg m^{-3})

Fig .3

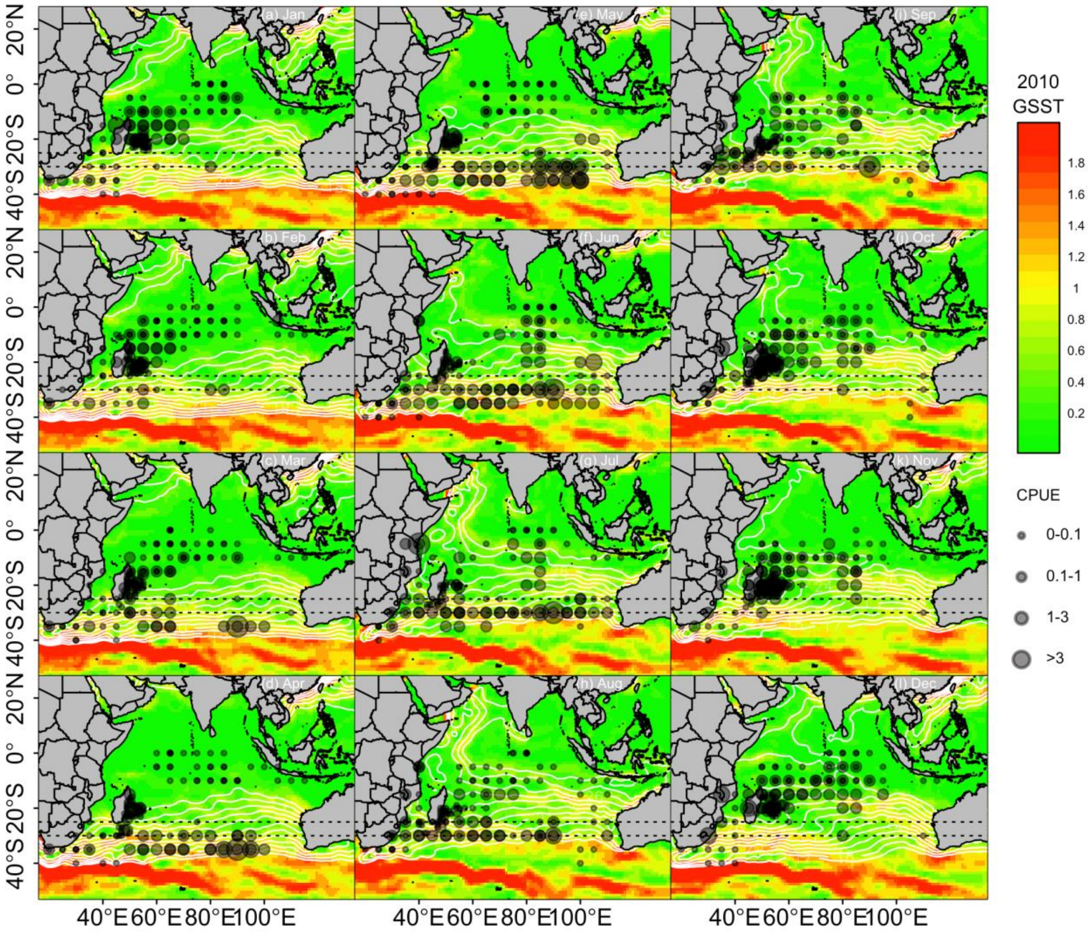
(a) Jan
(e) May
(i) Sep
(b) Feb
(f) Jun
(j) Oct
(c) Mar
(g) Jul
(k) Nov
(d) Apr
(h) Aug
(l) Dec
20°N
0°
20°S
40°S
40°E 60°E 80°E 100°E
2010
GSST
1.8
1.6
1.4
1.2
1
0.8
0.6
0.4
0.2
CPUE
0-0.1
0.1-1
1-3
>3

Fig. 4

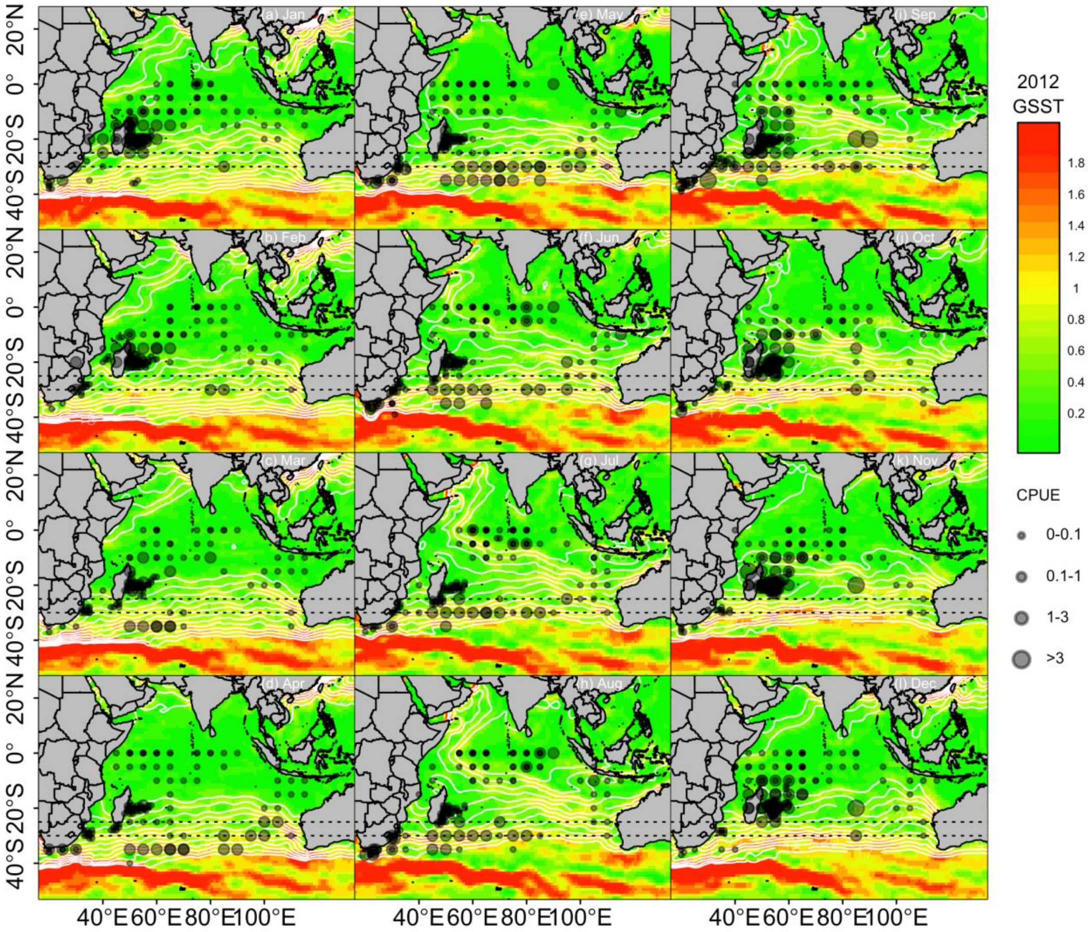
(a) Jan
(b) Feb
(c) Mar
(d) Apr
(e) May
(f) Jun
(g) Jul
(h) Aug
(i) Sep
(j) Oct
(k) Nov
(l) Dec
20°N
0°
20°S
40°S
40°E
60°E
80°E
100°E
2012
GSST
1.8
1.6
1.4
1.2
1
0.8
0.6
0.4
0.2
CPUE
0-0.1
0.1-1
1-3
>3

Fig. 5